Ishii et al. (2003) Inactivation of Integrin-linked Kinase Induces Aberrant Tau Phosphorylation via Sustained Activation of Glycogen Synthase kinase 3β in N1E-115 Neuroblastoma Cells., J. Biol. Chem. 278: 26970-26975.

Inactivation of Integrin-linked Kinase Induces Aberrant Tau Phosphorylation via Sustained Activation of Glycogen Synthase kinase 3β in N1E-115 Neuroblastoma Cells

Toshiaki Ishii*, Hidefumi Furuoka, Yoshikage Muroi, and Masakazu Nishimura

Department of Pathobiological Science, Obihiro University of Agriculture and Veterinary Medicine, Obihiro Hokkaido 080-8555, Japan

*Correspondence to: Dr. Toshiaki Ishii
Department of Pathobiological Science,
Obihiro University of Agriculture and
Veterinary Medicine,
Obihiro Hokkaido 080-8555, Japan
(Phone) +81-155-49-5366
(Fax) +81-155-49-5369
(E-mail) ishii@obihiro.ac.jp

Running title: Aberrant tau phosphorylation induced by ILK inactivation

Integrin-linked kinase (ILK) is a focal adhesion serine/threonine protein kinase with an important role in integrin- and growth factor-signaling pathways. Recently, we demonstrated that ILK is expressed in N1E-115 neuroblastoma cells and controls integrin-dependent neurite outgrowth in serum-starved cells grown on laminin (Ishii, T. et al.(2001) J. Biol. Chem. 276, 42994-43003). Here we report that ILK controls tau phosphorylation via regulation of glycogen synthase kinase-3β (GSK-3β) activity in N1E-115 cells. Stable transfection of a kinase-deficient ILK mutant (DN-ILK) resulted in aberrant tau phosphorylation in N1E-115 cells at sites recognized by the Tau-1 antibody, which are identical to some of the phosphorylation sites in paired helical filaments, (PHF)-tau, in brains of patients with Alzheimer's disease. The tau phosphorylation levels in the DN-ILK-expressing cells are constant under normal and differentiating conditions. On the other hand, aberrant tau phosphorylation was not observed in the parental control cells. ILK inactivation resulted in an increase in the active form but a decrease in the inactive form of GSK-3β, which is a candidate kinase involved in PHF-tau formation. Moreover, inhibition of GSK-3β with lithium prevented aberrant tau phosphorylation in the DN-ILK-expressing cells. These results suggest that ILK

inactivation results in aberrant tau phosphorylation via sustained activation of GSK-3β•in N1E-115 Cells. ILK directly phosphorylates GSK-3β and inhibits its activity. Therefore, endogenous ILK protects against GSK-3β-induced aberrant tau phosphorylation via inhibition of GSK-3β activity in N1E-115 cells.

Introduction

Tau is a microtubule-associated protein that stabilizes microtubules within neurites and axons (1). It is hypothesized that tau hyperphosphorylation leads to the destabilization of microtubules and aggregation of tau proteins, which impairs axonal transport and eventually results in neuronal-cell death (1-3). Indeed, tau hyperphosphorylation appears to be an early event preceding the formation of paired helical filaments (PHF) in the brains of Alzheimer's disease patients (4). On the other hand, tau phosphorylation seems also to control microtubule dynamics during neurite outgrowth and neuronal maturation because embryonic and neonatal tau is much more heavily phosphorylated than adult tau (5-8). Thus, the study of the regulation of tau phosphorylation in neurons is important for understanding the neurofibrillary degeneration in Alzheimer's disease as well as the physiologic function of tau in neurite outgrowth and neuronal

development.

Integrin-linked kinase (ILK) is a cytoplasmic serine/threonine kinase protein that serves as a mediator in integrin- and growth factor-mediated signal transduction (9,10). ILK is expressed in N1E-115 cells and controls integrin-dependent neurite outgrowth (11). In the present study, stable transfection of a kinase-deficient mutant of ILK (DN-ILK), which behaves as a dominant negative and inactivates endogenous ILK, resulted in aberrant tau phosphorylation. DN-ILK overexpression increased the active form and decreased the inactive form of GSK-3β. On the other hand, a selective uncompetitive inhibitor of GSK-3β, lithium, inhibited aberrant tau hyperphosphorylation. These results suggest that inactivation of ILK results in sustained activation of GSK-3β and leads to aberrant tau phosphorylation in N1E-115 neuroblastoma cells.

Experimental procedures

Reagents - LY294002 was obtained from Sigma Chemical Co. (St. Louis, MO). Rabbit polyclonal anti-ILK IgG (UB 06-550 and UB 06-592) and myelin basic protein were obtained from Upstate Biotechnology (Lake Placid, NY). Anti-GSK-3β antibody for immunoprecipitation was obtained from Transduction Laboratories (Lexington, KY). Anti-Tau-1 was obtained from Roche Molecular

Biochemicals (Tokyo, Japan). Anti-Tau, anti-phospho(Ser^{199},Ser^{202})-Tau, and anti-GSK-3β were obtained from Calbiochem (La Jolla, CA). Anti-phospho(Ser^{9})-GSK-3β and anti-phospho(Tyr^{279}/^{216})-GSK-3α/β were obtained from ABA (Golden, CO). Alexa Fluor (R) 488 goat anti-rabbit IgG was obtained from Molecular Probes (Eugene, OR). GSK-3β substrate (2B-SP) was obtained from Takara (custom synthesis service, Tokyo, Japan). All other chemicals were of analytical grade and were obtained from Sigma Chemical Co. or Wako Pure Chemical Co. (Osaka, Japan) unless otherwise specified.

Construction and Transfection of cDNA Vectors, and Cell Culture - Mouse N1E-115 neuroblastoma cells were maintained in Dulbecco's modified Eagle's medium (DMEM) containing 20% fetal bovine serum (FBS; Hyclone, Logan, UT). The kinase deficient ILK (DN-ILK) was generated by site-directed mutagenesis (Glu to Lys) at amino acid residue 359 within the kinase domain of wild type ILK (GenBank accession number AF256520) using polymerase chain reaction (PCR) as described previously (11). Wild-type ILK and DN-ILK cDNAs were ligated into the polylinkers in two different mammalian-expression vectors, pTracerTM-CMV2 (V885-01, Invitrogen Corp., Carlsbad, CA) and pRc-CMV (V750-20, Invitrogen

Corp.). The DN-ILK cDNA was transfected into N1E-115 cells (5 x 10^5 cells/100 mm culture dish) using the calcium/phosphate precipitation method as described by Graham and van der Eb (12), and 48 individual Zeocin - resistant cell lines were isolated over the next 4 to 5 wk. Among them, three different cell lines were selected based on the detection of green fluorecent protein (GFP) fluorescence and confirmation of gene transcription using reverse transcriptase (RT)-PCR. The cloned cell lines were maintained in DMEM containing 20% FBS and Zeocin (0.5 mg/ml).

ILK Assay - ILK assay was performed as described by Delcommenne et al. (13). Cells were lysed in 50 mM Hepes buffer (pH 7.5) containing 150 mM NaCl, 1% Nonidet P-40, 0.5% sodium deoxycholate, 10 µg/ml leupeptin, 2.5 µg/ml aprotinin, 1 mM phenylmethylsulfonyl fluoride (PMSF), 5 mM sodium fluoride, and 1 mM sodium orthovanadate. The lysates were incubated with anti-ILK antibody (UB 06-592) at 4°C for 12 h. After incubation, the lysates were precleared and immune complexes were collected with protein A-Sepharose. After washing twice with lysis buffer and once with 50 mM HEPES (pH 7.0) buffer containing 1 mM EDTA, the immunoprecipitated ILK was incubated for 20 min at 30°C in the presence or absence of 10 µg of the exogenous substrate myelin

basic protein in a total volume of 50 µl kinase reaction buffer (50 mM HEPES pH 7.0, 10 mM MnCl2, 10 mM MgCl2, 2 mM NaF, 1 mM Na3VO4) containing 6 µM [γ-^{32}P]ATP (10 µCi; NEG-502Z, Dupont NEN, Wilmington, DE). The reaction was stopped by the addition of an equal volume of 2x sodium dodecyl sulfate-polyacrylamide gel electrophoresis (SDS-PAGE) sample buffer. The kinase reaction products were analyzed using SDS-PAGE (5-20% polyacrylamide) and autoradiography. For detection of the immunoprecipitated ILK and DN-ILK proteins, the precipitated proteins were released from the immunobeads by boiling in 80 µl of SDS-PAGE sample buffer for 5 min. Equal volumes of the samples were loaded onto SDS-PAGE. Total ILK and DN-ILK proteins were detected by immunoblotting with an anti-ILK antibody (UB 06-550) that recognized both ILK and DN-ILK proteins.

GSK-3β Assay - GSK-3β assay was performed essentially as described by Cross (14). Cells were lysed in 50 mM Hepes buffer (pH 7.5) containing 150 mM NaCl, 1% Nonidet P-40, 5 mM sodium fluoride, 1 mM sodium orthovanadate, 5 mM EDTA, 100 nM okadaic acid, and protease inhibitors (Complete; Roche Diagnostics, Basel, Switzerland). The lysates were incubated with anti-GSK-3β antibody (Transduction Laboratories, Lexington, KY) at 4^{o}C for

1 h followed by overnight incubation with protein G-Sepharose. After washing twice with lysis buffer and once with 50 mM HEPES (pH 7.0) buffer containing 1 mM EDTA, the immunoprecipitated GSK-3β was incubated for 30 min at 30°C in the presence or absence of 4 μM specific substrate peptide 2B-SP [Ac-RRAAEELDSRAGS(p)PQL] in a total volume of 50 μl kinase reaction buffer (50 mM HEPES, pH 7.0, 10 mM MnCl2, 10 mM MgCl2, 2 mM NaF, 1 mM Na3VO4) containing 10 μM [γ-^{32}P]ATP (0.2 μCi; NEG-502Z, Dupont NEN, Wilmington, DE). The reaction was stopped by placing the samples on ice. After brief centrifugation, 25 μl of the reaction supernatant was spotted onto P81 phosphocellulose paper filters (Whatman, ME, UK), washed with 75 mM phosphoric acid, and rinsed with acetone. The amount of radioactive phosphate incorporated into substrate peptides was determined by scintillation counting.

Immunofluorescent Staining – Cells grown on Lab-Tek® chamber slides (Nunc, Tokyo, Japan) were fixed in 1% neutral buffered formaldehyde solution for 10 min and then permeabilized with 0.25% saponin in Hanks' balanced salt solution for 20 min. Permeabilized cells were incubated for 1 h in rabbit anti-phospho (Ser^{199}, Ser^{202})-Tau antibody (Calbiochem; final dilution 1:100 in phosphate buffered saline; PBS). After rinsing in PBS, the cells

were incubated for 1 h in Alexa Fluor (R) 488 goat anti-rabbit IgG (1: 100). Images were obtained by fluorescent microscopy (OLYMPUS; Tokyo, Japan) and confocal laser scanning microscopy (NIKON; Tokyo, Japan).

Antibodies – Anti-Tau (recognizes both native and phosphorylated forms of tau), anti-Tau-1 [recognizes tau dephosphorylated at Ser^{195}, Ser^{198}, Ser^{199}, Ser^{202}, and Thr^{205}(15,16)], and Anti-GSK-3β antibody for immunoprecipitation (Transduction Laboratories) were mouse monoclonal antibodies. All the other antibodies, anti-phospho (Ser^{199}, Ser^{202})-Tau (recognizes tau phosphorylated at Ser^{199} and Ser^{202}), anti-GSK 3β (recognizes both native and phosphorylated forms of GSK-3β), anti-phospho (Ser^{9})-GSK 3β (Affinity Bioreagents; recognizes GSK-3β phosphorylated at Ser^{9}), anti-phospho (Tyr^{279}/^{216})-GSK 3α/β (Affinity Bioreagents; recognizes GSK-3α and GSK-3β phosphorylated at Tyr^{279} and Tyr^{216}, respectively), and anti-ILK (Upstate Biotechnology; UB 06-550 for immunoblotting and UB 06-593 for immunoprecipitation) were rabbit polyclonal antibodies.

Western Blot Analysis- Cells were solubilized in 100 µl sample buffer containing 2% SDS, 10% glycerol, 50 mM dithiothreitol, 0.1%

bromophenol blue, and 62.5 mM Tris-HCl (pH6.8) after washing once with PBS. For detection of ILK expression, cells were solubilized in 5 volumes of buffer containing 1% Triton X-100, 150 mM NaCl, 50 mM Tris-HCl (pH 7.4), 5 mM EGTA, and 2 mM PMSF at 4°C. The solubilized materials were subjected to SDS-PAGE (5-20% gradient, 6.5% or 10% polyacrylamide) and transferred onto nitrocellulose membranes at 4°C in 25 mM Tris-HCl (pH 8.4), 192 mM glycine, 20% methanol, and 0.025% SDS. After blocking, the blots were probed with appropriate primary antibodies in Tris-buffered saline containing 0.05% Tween20, followed by goat anti-rabbit or goat anti-mouse IgG conjugated to horseradish peroxidase. The final protein/IgG complexes were visualized following the reaction to 3,3'-diaminobenzidine tetrahydrochloride.

Results

DN-ILK Inhibits Basal ILK Activity and Prevents Stimulation of ILK Activity after Cell Adhesion on Laminin under Serum-free Condition - Mouse N1E-115 neuroblastoma cells grown on a laminin matrix exhibit neurite outgrowth in response to serum deprivation (11,17). We have previously demonstrated that ILK is expressed in N1E-115 neuroblastoma cells and controls integrin-dependent neurite outgrowth in serum-starved cells grown on laminin (11). To inactivate endogenous ILK, cells were stably transfected with

DN-ILK, which behaves as a dominant negative (11,13). Based on the results obtained from immunoblotting (Fig.1), the expression level of DN-ILK protein in DN-ILK-transfected cells was estimated to be at least twice that of endogenous ILK protein and neither the ILK nor DN-ILK expression level changed under differentiating conditions. The ILK activity in the parental cells under serum-free conditions was transiently activated after seeding on the laminin matrix, whereas that in the DN-ILK-transfected cells was not. Also, weak basal ILK activity was detected only in the parental cells under non-differentiating conditions (Fig.1). These findings are consistant with our previous observations (11). Thus, DN-ILK inactivates endogenous ILK under both differentiating and non-differentiating conditions.

Inactivation of Endogenous ILK Induces aberrant Tau phosphorylation - To examine whether tau phosphorylation is involved in neurite outgrowth in N1E-115 cells, we analyzed the tau phosphorylation level in parental and DN-ILK-transfected cells using phosphorylation- and dephosphorylation-dependent anti-tau antibodies. Western blots of tau from both parental and DN-ILK-transfected cells were probed with three different tau antibodies, anti-Tau-1, which recognizes an epitope of tau only when it is not phosphorylated, anti-Phospho (Ser^{199}, Ser^{202})-Tau,

which recognizes tau phosphorylated at Ser^{199} and Ser^{202}, and anti-Tau, which recognizes both native and phosphorylated forms of tau. In non-transfected parental cells, tau was recognized by anti-Tau-1 but not anti-Phospho (Ser^{199}, Ser^{202})-Tau antibody, under both normal and differentiating conditions. Thus, tau in the parental cells was not phosphorylated at sites recognized by those antibodies in either condition. On the other hand, cells stably transfected with a DN-ILK to inactivate the endogenous ILK had dramatically decreased anti-Tau-1 immunoreactivity but an increased anti-Phospho (Ser^{199}, Ser^{202})-Tau immunoreactivity (Fig.1). Thus, tau was phosphorylated in DN-ILK-transfected cells and the tau phosphorylation level did not change even under differentiating conditions. Total tau detected with anti-Tau antibody migrated as several bands in the 40 to 70-kDa range, but some of the protein bands, which migrate relatively slower on SDS-PAGE, were weaker when tau was phosphorylated (Fig.1). These results suggest that inactivation of endogenous ILK results in aberrant hyperphosphorylation of tau, at least at Ser^{199} and Ser^{202}.

Immunofluorescent Staining of Aberrantly Phosphorylated Tau – To examine the intracellular localization of aberrantly phosphorylated tau, cells were stained with antibody against phosphorylated tau. Immunofluorescent staining of cell

monolayers with anti-Phospho (Ser^{199}, Ser^{202})-Tau antibody is shown in Fig. 2. DN-ILK-transfected cells were strongly stained with the antibody against phosphorylated tau under normal and differentiating conditions. On the other hand, parental cells were not significantly stained under differentiating conditions, but very weak dot-like structures were observed only in the non-differentiated cells, suggesting that a small minority of the tau, which could not be detected by the immunoblotting analysis, might be phosphorylated under non-differentiating conditions. In the DN-ILK-transfected cells, intracellular cytoplasm, except the nucleus, was stained with strong immunofluorescent intensity and microtubule-like structures were observed. Further analysis of the DN-ILK-transfected cells using confocal laser scanning microscopy indicated that microtubule-like structures spread and cover right under the whole plasma membrane of the cells, and form basket-like structures (Fig.2 *inset* left and right).

Active Form of GSK-3β Increases in DN-ILK-transfected Cells - To examine signal pathways involved in tau phosphorylation, we analyzed the activation status of GSK-3β, because GSK-3β is one of the candidate kinases that can phosphorylate tau at both Ser^{199} and Ser^{202} (18), and also has an important role in the ILK-mediated signal pathway (13,19,20). Activation of GSK-3β is dependent on

Tyr^{216} phosphorylation (21). On the other hand, GSK-3β activity is inhibited by direct phosphorylation at Ser^{9} by ILK (20,22) and by protein kinase B (PKB)/Akt, which is also activated via ILK (13,23). We, therefore, examined whether the levels of these phosphorylated GSK-3β forms are different between parental and DN-ILK-transfected cells and are changed under different culture conditions by Western blot analysis using anti-phospho (Ser^{9})-GSK-3β and anti-phospho ($Tyr^{279}/^{216}$)-GSK-3α/β antibodies. Tyr^{216} in GSK-3β was highly phosphorylated in DN-ILK-transfected cells but was very weakly phosphorylated in parental cells (Fig.3A). In contrast, Ser^{9} in GSK-3β was highly phosphorylated in parental cells but not in DN-ILK-transfected cells. Moreover, these phosphorylation levels were not significantly different between non-differentiating and differentiating conditions. The expression level of GSK-3β was not different among all cells tested. These results suggest that ILK inactivation results in Ser^{9} dephosphorylation and increased Tyr^{216} phosphorylation in GSK-3β, thereby activating the enzyme.

GSK-3β Activity Is Activated by Inactivation of Endogenous ILK in DN-ILK-transfected Cells – To test whether the level of GSK-3β activity increases in DN-ILK-transfected cells, we performed a GSK-3β kinase assay on proteins immunoprecipitated

from cell lysates with a monoclonal GSK-3β antibody. The level of GSK-3β activity in DN-ILK-transfected cells was approximately three times more than that in parental cells (Fig. 3B). The level of GSK-3β activity was not different between differentiating and non-differentiating conditions in either DN-ILK-transfected or parental cells (Fig. 3B). Thus, inactivation of endogenous ILK results in increased GSK-3β activity. This result is consistent with the fact that ILK inactivation induced an increase in the levels of active GSK-3β formed via Tyr^{216} phosphorylation (Fig. 3A).

Lithium Reduces Tau Phosphorylation in A Dose-dependent Manner - Lithium is an uncompetitive GSK-3β inhibitor (24). We therefore examined the effect of lithium on tau phosphorylation. Cells were treated with varying concentrations of LiCl for 16 h under non-differentiating conditions. Treatment of DN-ILK-transfected cells with LiCl reduced anti-phospho (Ser^{199}, Ser^{202})-Tau immunoreactivity, but increased anti-Tau-1 immunoreactivity in a dose-dependent manner (Fig.4). Moreover, reaction of slowly migrated tau bands with anti-Tau, which were supposed to be non-phosphorylated tau, were recovered after treatment with LiCl in a dose-dependent manner. The same results were obtained in DN-ILK-transfected cells under differentiating

conditions (data not shown). These results suggest that LiCl inhibited tau phosphorylation at Ser^{199} and Ser^{202}, and also at the sites recognized by anti-Tau-1. On the other hand, the same treatment of parental cells with 25 mM LiCl did not affect either anti-Tau-1 or anti-phospho (Ser^{199}, Ser^{202})-Tau immunoreactivity. These results suggest that GSK-3β activation induced by ILK inactivation is directly involved in tau phosphorylation at Ser^{199} and Ser^{202}, and also at the sites recognized by anti-Tau-1.

Aberrant Tau phosphorylation Is Partly Involved in Inhibition of Neurite Outgrowth in DN-ILK-transfected Cells – We previously demonstrated that activation of p38 mitogen-activated protein (MAP) kinase is involved in ILK-mediated signal transduction leading to integrin-dependent neurite outgrowth in N1E-115 cells (11). In the previous report, we suggested that signaling pathways other than p38 MAP kinase, which is also activated via ILK activation, might be involved in integrin-dependent neurite outgrowth, because a p38 MAP kinase inhibitor, SB203580, blocked approximately 80% of the ILK-dependent neurite outgrowth (11, also see Fig.5). To examine whether aberrant tau phosphorylation is involved in the inhibition of neurite outgrowth in DN-ILK-transfected cells, we treated the cells with 10 mM LiCl, a dose that prevents aberrant

tau phosphorylation, under serum-free conditions. Treatment of the DN-ILK-transfected cells with LiCl partially recovered neurite outgrowth, in the presence or absence of SB203580, to the levels of that in the SB20358-treated parental cells (Fig.5). On the other hand, treatment of the parental cells with LiCl did not affect neurite outgrowth in either the presence or absence of SB203580 (Fig.5). These results suggest that aberrant tau phosphorylation is partly involved in the inhibition of neurite outgrowth in DN-ILK-transfected cells.

Discussion

The present study demonstrates that ILK inactivation induces aberrant tau phosphorylation via GSK-3β activation in N1E-115 cells, which is partly involved in the inhibition of neurite outgrowth, based on the following observations: 1) tau was phosphorylated at Ser^{199} and Ser^{202}, and at the sites recognized by anti-Tau-1 in DN-ILK transfected cells but not in parental cells, 2) ILK inactivation increased the active form, but decreased the inactive form of GSK-3β, leading to increased GSK-3β activity, and 3) treatment of the DN-ILK-transfected cells with LiCl, an uncompetitive inhibitor of GSK-3β, blocked aberrant tau phosphorylation and partly recovered the levels of neurite

outgrowth in DN-ILK-transfected cells.

Integrin signaling is required for neurogenesis in serum-starved N1E-115 cells (25). N1E-115 cells grown on a laminin matrix exhibit neurite outgrowth in response to serum deprivation (11,17). This neurite outgrowth depends on an integrin-dependent signal pathway, because pre-treatment of cells with anti-β1 integrin antibody inhibited neurite outgrowth (11,17). We recently demonstrated that ILK is expressed in N1E-115 cells and controls integrin-dependent neurite outgrowth in serum-starved cells grown on laminin (11). In the present study, stable transfection of DN-ILK, which behaves as a dominant negative and inactivates endogenous ILK, resulted in aberrant tau phosphorylation. On the other hand, the aberrant tau phosphorylation was not observed in the parental cells under either normal or differentiating conditions. ILK activity in the parental cells was increased after seeding on the laminin matrix under serum-free conditions, whereas that in the DN-ILK-transfected cells was not. Thus, both cell adhesion to laminin and serum-deprivation were necessary for full activation of ILK. On the other hand, weak basal ILK activity was detected in the parental cells under non-differentiating normal conditions (Fig.1). It remains unknown how basal ILK activity is maintained

under non-differentiation. These results suggest that endogenous ILK prevents aberrant tau phosphorylation. Moreover, aberrant tau phosphorylation did not significantly occur in the parental cells under normal conditions, suggesting that weak basal ILK activity is sufficient to protect tau from aberrant phosphorylation.

To examine whether aberrantly phosphorylated tau participates in microtubule formation, we stained cells with antibody against phosphorylated tau (Fig. 2). Intracellular cytoplasm, except for the nucleus, was stained with strong immunofluorescent intensity and microtubule-like structures were observed only in DN-ILK-transfected cells. Moreover, analysis of the DN-ILK-transfected cells using confocal laser scanning microscopy indicated that microtubule-like structures spread and cover right under the whole plasma membrane of the cells, and form basket-like structures (Fig.2 *inset* left and right). Thus, aberrantly phosphorylated tau participates in microtubule-like structures but is located only immediately under the plasma membrane in the cytosol without being able to form neurites in DN-ILK-transfected cells. On the other hand, parental control cells under non-differentiating conditions were very weakly stained with antibodies against phosphorylated tau, which could not be detected by the immunoblotting analysis, but

neurite-bearing control cells under differentiating conditions were not (Fig. 2, a and c). These results suggest that tau phosphorylation at Ser^{199} and Ser^{202} might negatively control microtubule rearrangement necessary for neurite outgrowth via microtubule instability.

Tau is phosphorylated at Ser^{199} and Ser^{202}, and at the sites recognized by anti-Tau-1, which correspond to Ser^{195}, Ser^{198}, Ser^{199}, Ser^{202}, and Thr^{205}. Ser^{199} and Ser^{202} are phosphorylated by GSK-3β (18), which is a candidate kinase involved in PHF-tau formation (26,27). Moreover, GSK-3β has an important role in the ILK-mediated signal pathway (10,19). We, therefore, examined the involvement of GSK-3β in aberrant tau phosphorylation in DN-ILK-transfected cells. Activation of GSK-3β is dependent upon the Tyr^{216} phosphorylation (21). On the other hand, GSK-3β activity is inhibited by direct Ser^{9} phosphorylation by ILK (19,22) and by protein kinase B (PKB)/Akt whose activity is also activated via ILK (13,23). Tyr^{216} in GSK-3β was highly phosphorylated in DN-ILK-transfected cells but was very weakly phosphorylated in parental cells. In contrast, Ser^{9} in GSK-3β was highly phosphorylated in parental cells but not in DN-ILK-transfected cells. These phosphorylation levels were not significantly different between non-differentiating and differentiating

conditions (Fig.3A). Thus, GSK-3β was phosphorylated at both Ser^{9} and Tyr^{216} in parental cells, while Tyr^{216} phosphorylation was considerably lower (Fig.3A). Recently, Bhat et al. (2000) (28) suggested that Ser^{9} phosphorylation is sufficient to override the Tyr^{216} phosphorylation-induced activation of GSK-3β. Therefore, the level of GSK-3β activity seems to maintain lower via Ser^{9} phosphorylation in parental cells. These results suggest that ILK inactivates GSK-3β via phosphorylation at Ser^{9} and prevents activation. In contrast, ILK inactivation results in Ser^{9} dephosphorylation and increased Tyr^{216} phosphorylation in GSK-3β, thereby activating the enzyme. Indeed, the level of GSK-3β activity in DN-ILK-transfected cells was significantly higher than that in parental cells (Fig. 3B).

Lithium, a selective uncompetitive inhibitor of GSK-3β (24), inhibited tau phosphorylation at Ser^{199} and Ser^{202}, and also at the sites recognized by anti-Tau-1 in a dose-dependent manner (Fig.4). These results suggest that GSK-3β activation induced by ILK inactivation is directly involved in tau phosphorylation at Ser^{199} and Ser^{202}, and also at the sites recognized by anti-Tau-1. As both Ser^{199} and Ser^{202} are phosphorylated by GSK-3β(18), GSK-3β at least directly phosphorylates these Ser residues in the DN-ILK-transfected cells. Although a specific tyrosine kinase,

which should be activated by ILK inactivation, is probably involved in the Tyr^{216} phosphorylation in GSK-3β, we have not yet determined the kinase involved in this study. To understand the ILK-mediated regulatory mechanisms of GSK-3β, the specific tyrosine kinase that is activated by ILK inactivation and phosphorylates Tyr^{216} in GSK-3β must be determined.

We previously demonstrated that p38 MAP kinase in the ILK-mediated signal pathway has an important role in integrin-dependent neurite outgrowth in N1E-115 cells (11). On the other hand, a p38 MAP kinase inhibitor, SB203580, blocked approximately 80% of the ILK-dependent neurite outgrowth, but not to the levels of the DN-ILK–transfected cells(11, also see Fig.5). In the previous study, we suggested that signaling pathways other than p38 MAP kinase, which are also activated via ILK activation, are involved in integrin-dependent neurite outgrowth (11). We therefore examined whether aberrant tau phosphorylation is involved in the inhibition of neurite outgrowth in DN-ILK-transfected cells. Treatment of the DN-ILK-transfected cells with 10 mM LiCl completely prevented aberrant tau phosphorylation but only partially recovered neurite outgrowth to the levels of that in the SB20358-treated parental cells. These results suggest that aberrant tau phosphorylation is partly

involved in the inhibition of neurite outgrowth in DN-ILK-transfected cells. Furthermore, the results also suggest that a p38 MAP kinase pathway is the sole downstream pathway in ILK-dependent neurite outgrowth.

Tau hyperphosphorylation decreases the association of tau with microtubules (29) and inhibits total neurite number (30-32). The inhibitory effect of aberrant tau phosphorylation on neurite outgrowth was as expected. The effect of aberrant tau phosphorylation, however, is considered to depend on the tau phosphorylation level and also on the number of phosphorylated tau molecules. While we could not estimate how many molecules in total tau are phosphorylated in the DN-ILK-transfected cells in this study, it is possible that the aberrant tau phosphorylation induced by ILK inactivation at least affects microtubule stability or dynamics and leads to inhibition of neurite outgrowth. On the other hand, endogenous ILK protects tau from aberrant phosphorylation and probably maintains a kind of equilibrium status responsible for microtubule reorganization. Thus, ILK is not only involved in p38 MAP kinase activation, but might also control microtubule dynamics via regulation of GSK-3β activity during neurite outgrowth in N1E-115 cells (Fig. 6). A recent study of NGF-induced neurite outgrowth using pheochromocytoma (PC12)

cells demonstrated that ILK is involved in NGF-induced neurite outgrowth via inhibition of tau hyperphosphorylation (33). This recent report using PC12 cells and our results obtained using N1E-115 cells suggest that ILK is an important regulator of both integrin- and growth factor-mediated signaling in neurons and controls neurite outgrowth. Moreover, ILK might be critical for the regulation of microtubule stability and rearrangement necessary for integrin- and growth factor-mediated neurite outgrowth.

References

1. Lovestone, S. and Reynolds, C.H. (1997) *Neuroscience* **78**, 309-324

2. Goedert, M., Spillanti, M.G., and Davies, S.W. (1998) *Curr. Opin. Neurobiol.* **8**, 619-632

3. Wang, J.Z., Grundke-Iqbal, I., and Iqbal, K. (1996) *Nat. Med.* **2**, 850-852

4. Bancher, C., Brunner, C., Lassmann, H., Budka, H., Jellinger, K., Wiche, G., Seitelberger, F., Grundke-Iqbal, I., Iqbal, K., and Wisniewski, H.M. (1989) *Brain Res.* **477**, 90-99

5. Bramblett, G.T., Goedert, M., Jakes, R., Merrick, S.E., Trojanowski, J.Q., and Lee, V.M.-Y. (1993) *Neuron* **10**, 1089-1099

6. Goedert, M., Jakes, R., Crowther, R.A., Six, J., Lubke, U., Vandermeeren, M., Cras, P., Trojanowski, J.Q., and Lee, V.M.-Y. (1993) *Proc. Natl. Acad. Sci. USA* **90**, 5066-5070

7. Matsuo, E.S., Shin, R.-W., Billingsley, M.L., Van deVoorde, A., O'Connor, M., Trojanowski, J.Q., and Lee, V.M.-Y. (1994) *Neuron* **13**, 989-1002

8. Burack, M.A., and Halpain, S. (1996) *Neuroscience* **72**, 167-184

9. Dedhar, S., Williams, B., and Hannigan, G. (1999) *Trends Cell Biol.* **9**, 319-323

10. Huang, Y., and Wu, C. (1999) *Int. J. Mol. Med.* **3**, 563-572

11. Ishii, T., Satoh, E., and Nishimura, M. (2001) *J. Biol. Chem.* **276**, 42994-43003

12. Graham, F.L., and van der Eb, A.J. (1973) *Virology* **52**, 456-467

13. Delcommenne, M., Tan, C., Gray, V., Rue, L., Woodgett, J., and Dedhar, S. (1998) *Proc. Natl. Acad. Sci. USA* **95**, 11211-11216

14. Cross, D. (2001) *Methods Mol. Biol.* **124**, 147-159

15. Binder, L.I., Frankfurter, A., and Rebhun, L.I. (1985) *J. Cell Biol.* **101**, 1371-1378

16. Szendrei, G.I., Lee, V.M., and Otvos, L.Jr. (1993) *J. Neurosci. Res.* **34**, 243-249

17. Sarner, S., Kozma, R., Ahmed, S., and Lin, L. (2000) *Mol. Cell. Biol.* **20**, 158-172

18. Liu, F., Iqbal, K., Grundke-Iqbal, I., Gong, C. (2002) *FEBS Lett.* **530**, 209-214

19. Troussard, A.A., Tan, C., Yoganathan, T.N., and Dedhar, S. (1999) *Mol. Cell. Biol.* **19**, 7420-7427

20. Persad, S., Troussard, A.A., McPhee, T.R., Mulholland, D.J., and Dedhar, S. (2001) *J. Cell Biol.* **153**, 1161-1173

21. Hughes, K., Nikolakaki, E., Plyte, S.E., Totty, N.F., and Woodgett, J.R. (1993) *EMBO J.* **12**, 803-808

22. Stambolic, V., and Woodgett, J.R. (1994) *Biochem. J.* **303**, 701-704

23. Persad, S., Attwell, S., Gray, V., Mawji, N., Deng, J.T., Leung, D., Yan, J., Sanghera, J., Walsh, M.P., and Dedhar, S. (2001) *J. Biol. Chem.* **276**, 27462-27469

24. Klein, P.S., and Melton, D.A. (1996) *Proc. Natl. Acad. Sci. USA* **93**, 8455-8459

25. van Leeuwen, F.N., Kain, H.E.T., van der Kammen, R.A., Michiels, F., Kranenburg, O.W., and Collard, J.G. (1997) *J. Cell Biol.* **139**, 797-807

26. Lovestone, S., Reynolds, C.H., Latimer, D., Davis, D.R., Anderton, B.H., Gallo, J.M., Hanger, D., Mulot, S., Marquardt, B., Stabel, S., Woodgett, J.R., and Miller, C.C.J. (1994) *Curr. Biol.* **4**, 1077-1086

27. Wagner, U., Utton, M., Gallo, J.-M., and Miller, C.C.J. (1996) *J. Cell Sci.* **109**, 1537-1543

28. Bhat, R.V., Shanley, J., Correll, M.P., Fieles, W.E., Keith, R.A., Scott, C.W., and Lee, C.-M. (2000) *Proc. Natl. Acad. Sci. USA* **97**, 11074-11079

29. Hong, M., and Lee, V.M.-Y. (1997) *J. Biol. Chem.* **272**, 19547-19553

30. Cressman C.M., and Shea, T.B. (1995) *J. Neurosci, Res.* **42**, 648-656

31. Malchiodi-Albedi, F., Petrucci, T.C., Picconi, B., Iosi, F., and Falchi, M. (1997) *J. Neurosci. Res.* **48**, 425-438

32. Sayas, C.L., Moreno-Flores, M.T., Avila, J., and Wandosell, F. (1999) *J. Biol. Chem.* **274**, 37046-37052

33. Mills, J., Digicaylioglu, M., Legg, A.T., Young, C.E., Young, S.S., Barr, A.M., Fletcher, L., O'Connor, T.P., and Dedhar, S. (2003) *J. Neurosci.* **23**, 1638-1648

Footnotes

The abbreviations used are: ILK, integrin-linked kinase; GSK-3β, glycogen synthase kinase 3β; DN, dominant negative; MAP, mitogen-activated protein; PHF, paired helical filaments; PAGE, polyacrylamide gel electrophoresis; FBS, fetal bovine serum; DMEM,

Dulbecco's modified Eagle's medium; NGF, nerve growth factor; PCR, polymerase chain reaction.

Key words: Integrin-linked kinase, N1E-115 cell, Neurite outgrowth, GSK-3β, Aberrant tau phosphorylation, Integrin.

Acknowledgements: We thank Dr. M. Niinobe (Institute for Protein Research, Osaka University, Japan) for providing the N1E-115 cells. This work was supported in part by a Grant-in-Aid for Scientific Research (C)(to T.I.) from the Japanese Ministry of Education, Science and Culture, in part by The Naito Foundation (to T.I.), and in part by The Akiyama Foundation (to T.I.).

Fig. 1. **Inactivation of endogenous ILK induces aberrant tau phosphorylation**. Cells were cultured for 16 h under either differentiating (seeding on laminin-coated plates in the absence of FBS) or non-differentiating (seeding on non-coated plates in the presence of FBS) conditions. Aberrant phosphorylation level of tau in parental and DN-ILK-transfected cells was detected by immunoblotting with an anti-Tau-1 antibody, which recognizes only a non-phosphorylated epitope of tau, and an anti-phospho (Ser^{199}, Ser^{202})-Tau antibody, which recognizes tau phosphorylated at Ser^{199},

Ser^{202}. Total tau was detected by an anti-Tau antibody, which recognizes both native and phosphorylated tau.

For the ILK assay and detection of ILK and DN-ILK proteins, cells were cultured for 60 min, which was required for maximal activation of ILK activity (11), under either differentiating or non-differentiating conditions and then lysed. ILK was immunoprecipitated from cell extracts. ILK activity was determined using myelin basic protein as an exogenous substrate, as described under “Experimental Procedures”. ILK and DN-ILK expression levels in cell lysates (20 μg) were analyzed using immunoblotting with an affinity-purified polyclonal anti-ILK antibody.

Fig. 2. **Subcellular localization of aberrantly phosphorylated tau at Ser^{199} and Ser^{202}**. After cells were cultured for 16 h under either differentiating (a and b) or non-differentiating (c and d) conditions, cells were stained with anti-phospho (Ser^{199}, Ser^{202})-Tau antibody, as described under “Experimental Procedures”. In DN-ILK-transfected cells, the intracellular cytoplasm, except for the nucleus, was strongly stained with the antibody and microtubule-like structures were observed under normal and differentiating conditions (b and d). On the other hand, parental

cells were not significantly stained under differentiating conditions (c) but very weak dot-like structures were observed in the non-differentiated cells (a). *Inset* shows further analysis of the DN-ILK-transfected cells using the confocal laser scanning microscopy. Microtubule-like structures spread and covered immediately under the whole plasma membrane of the cells, and formed basket-like structures (*inset* left and right).

Fig. 3. **Inactivation of endogenous ILK in DN-ILK-transfected cells results in a sustained increase in GSK-3β activity**. Cells were cultured for 16 h under either differentiating or non-differentiating conditions. *A*, the levels of an active form and an inactive form of GSK-3β were analyzed by immunoblotting with anti-phospho (Tyr^{279}/^{216})-GSK-3α/β and anti-phospho (Ser^{9})-GSK-3β antibodies, respectively. Total GSK-3β proteins were detected by immunoblotting with anti-GSK-3β antibody. *B*, GSK-3β activity was measured by immunoprecipitation followed by a kinase assay, as described under “Experimental Procedures”. The level of GSK-3β activity in DN-ILK-transfected cells was approximately three times more than that in parental cells under both culture conditions. Values are the means ± SD of four separate experiments.

Fig. 4. **Aberrant tau phosphorylation was prevented by treatment of cells with LiCl, an uncompetitive inhibitor of GSK-3β.** Cells were treated with varying concentrations of LiCl for 16 h under non-differentiating conditions. The level of aberrant tau phosphorylation was analyzed by immunoblotting with both anti-Tau-1 and anti-phospho (Ser^{199}, Ser^{202})-Tau antibodies. Total tau proteins were detected by immunoblotting with anti-Tau antibody, which recognizes both native and phosphorylated tau.

Fig. 5. **Effects of aberrant tau phosphorylation on neurite outgrowth in DN-ILK-transfected cells.** Cells were seeded on laminin-coated plates in serum-free medium in the presence of SB203580, LiCl, or LiCl plus SB203580. Treatment with only SB203580 was conducted for 3 h after seeding the cells by removing and changing the culture medium. The number of cells possessing neurites greater than twice the length of a cell body was assessed 16 h after plating the cells. Values are the means ± SD of four separate experiments. Statistical significance was determined using Student's *t*-test; a indicates $p<0.01$ (vs. non-treatment), b indicates $p<0.01$ (vs. 10 mM LiCl), c indicates $p<0.01$ (vs. non-treatment), and d indicates $p<0.05$ (vs. 10 μM SB203580).

Fig. 6. **Schematic model of aberrant tau phosphorylation in DN-ILK-transfected N1E-115 cells.** ILK is activated after cell adhesion on laminin in serum-free conditions in a PI3 kinase-dependent manner. Stimulation of ILK activity results in activation of p38 MAP kinase activity, which is important for ILK-dependent neurite outgrowth in N1E-115 cells (11). ILK phosphorylates GSK-3β at Ser^{9}, leading to GSK-3β inactivation. GSK-3β inactivation results in inhibition of aberrant tau phosphorylation, an increase in microtubule stability, and induces neurite outgrowth in combination with p38 MAP kinase action. On the other hand, ILK inactivation by DN-ILK induces GSK-3β phosphorylation at Tyr^{216} via activation of an unidentified tyrosine kinase, leading to GSK-3β activation. GSK-3β activation results in aberrant tau phosphorylation, microtubule instability, and decreased neurite outgrowth.

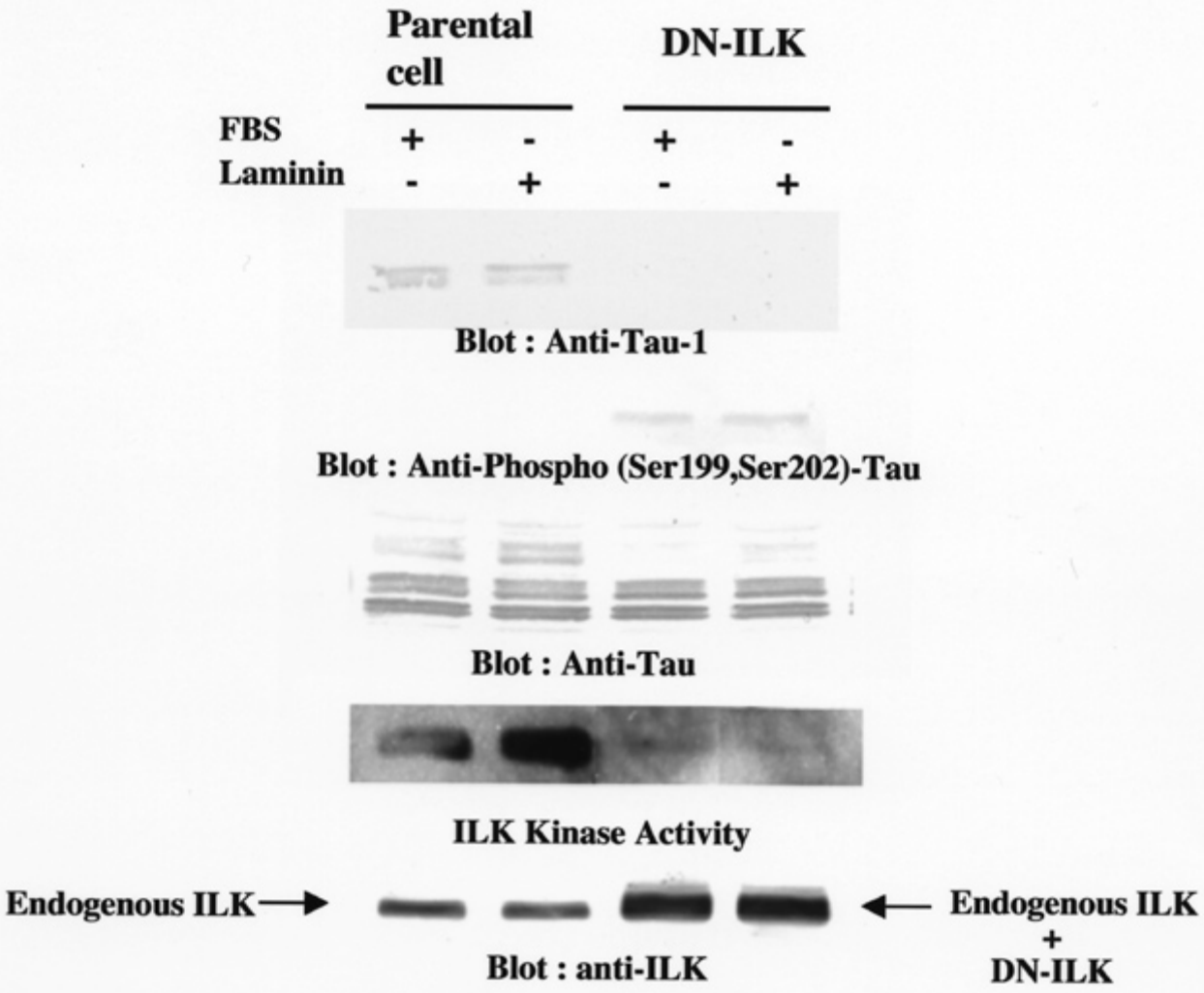

Ishii et al. Fig.1

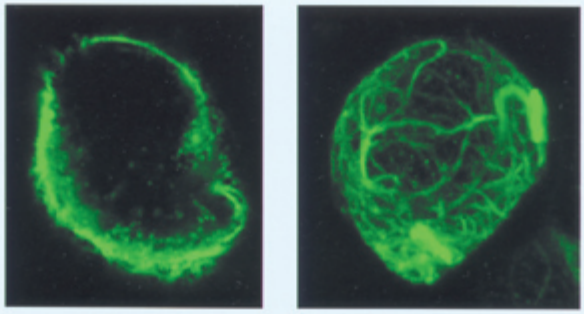

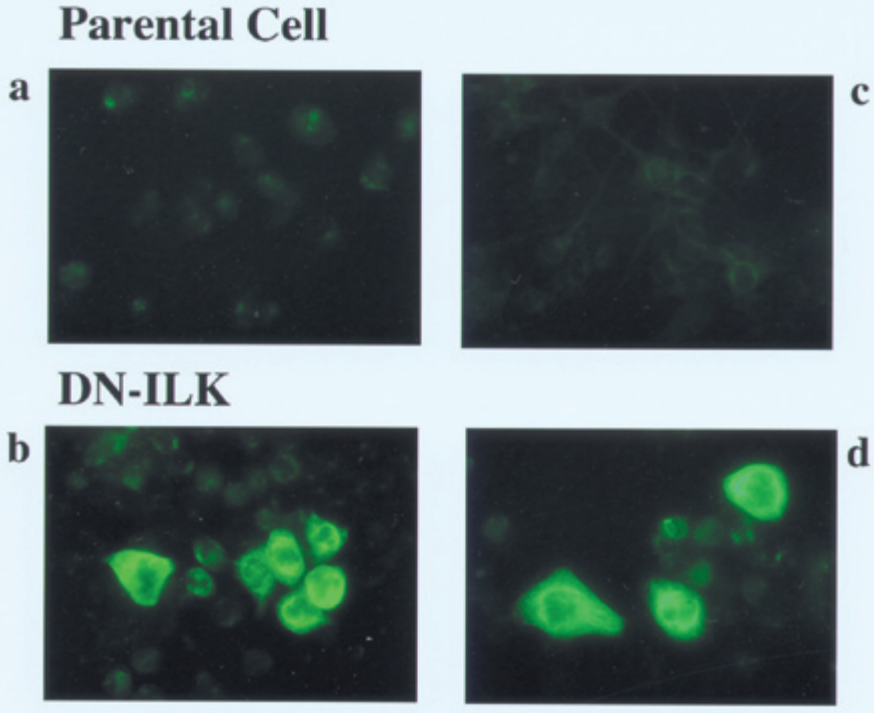

Ishii et al. Fig. 2

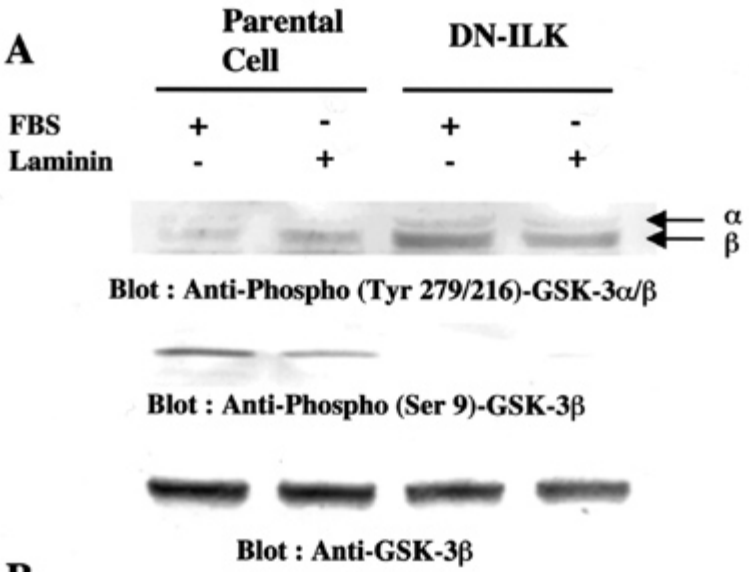

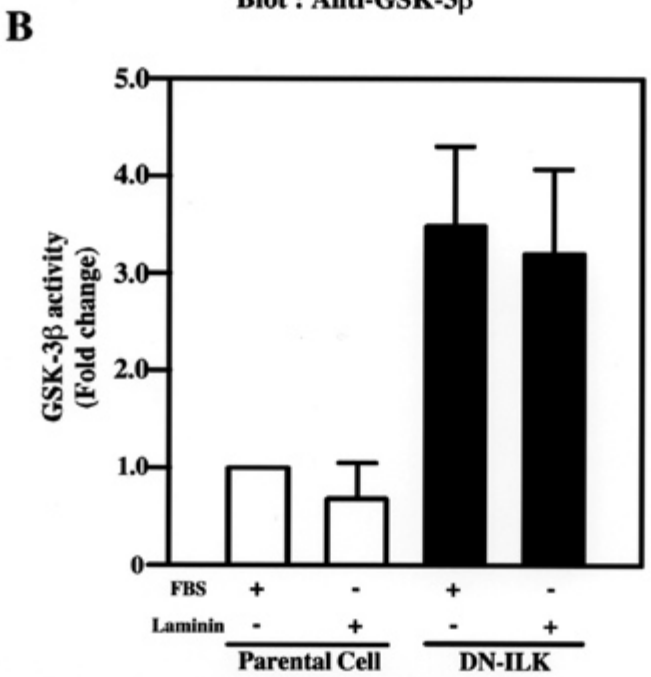

Ishii et al. Fig. 3

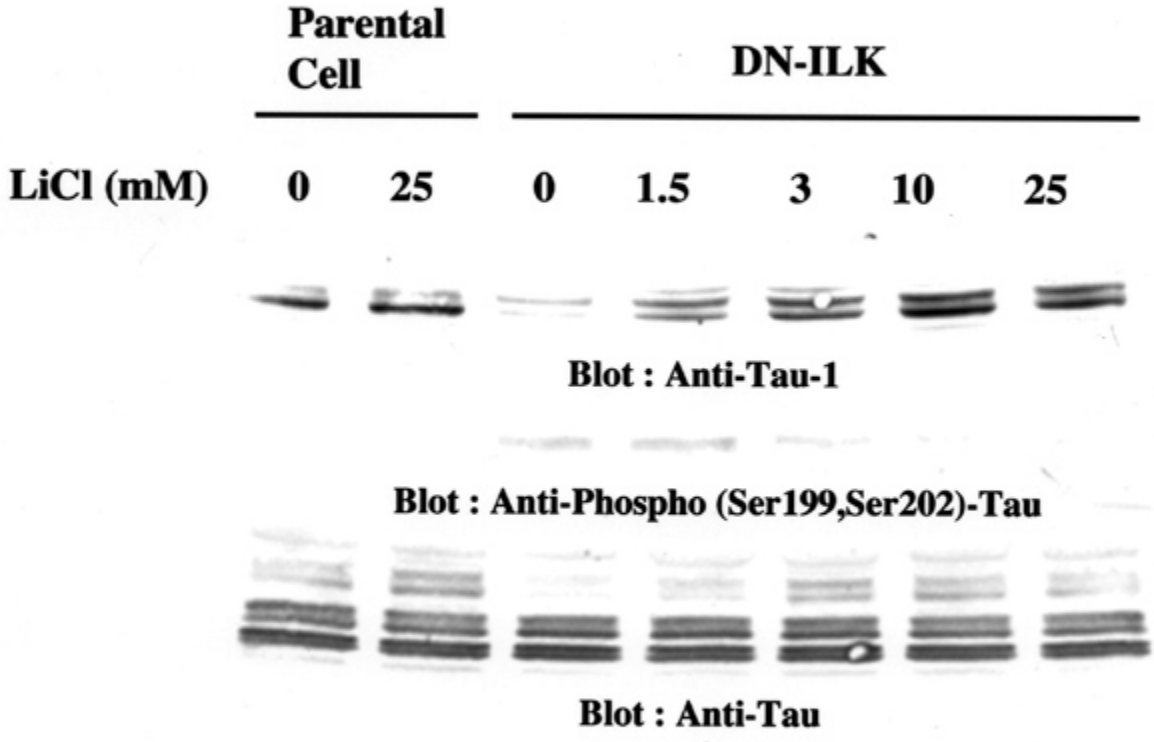

Ishii et al. Fig. 4

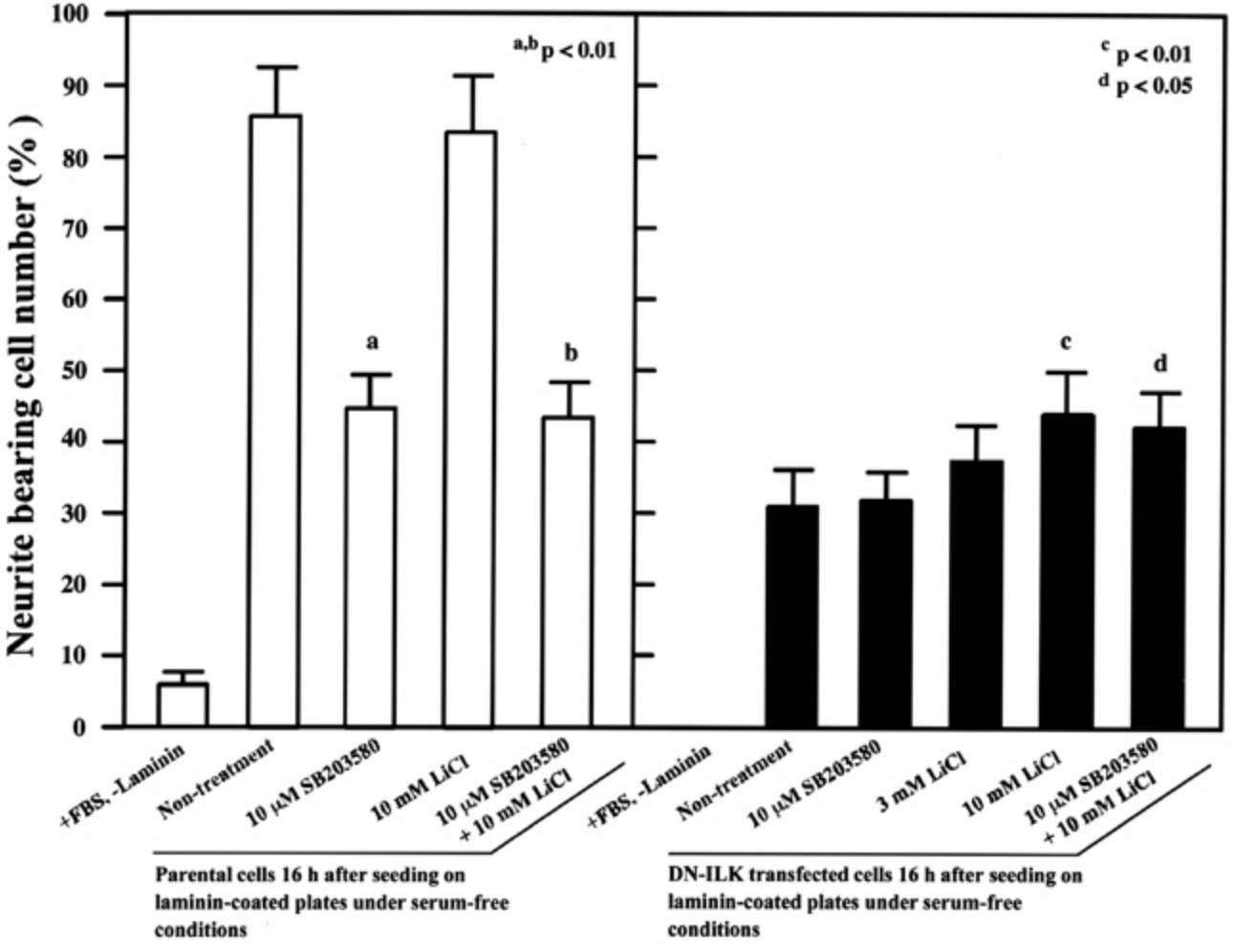

Ishii et al. Fig. 5

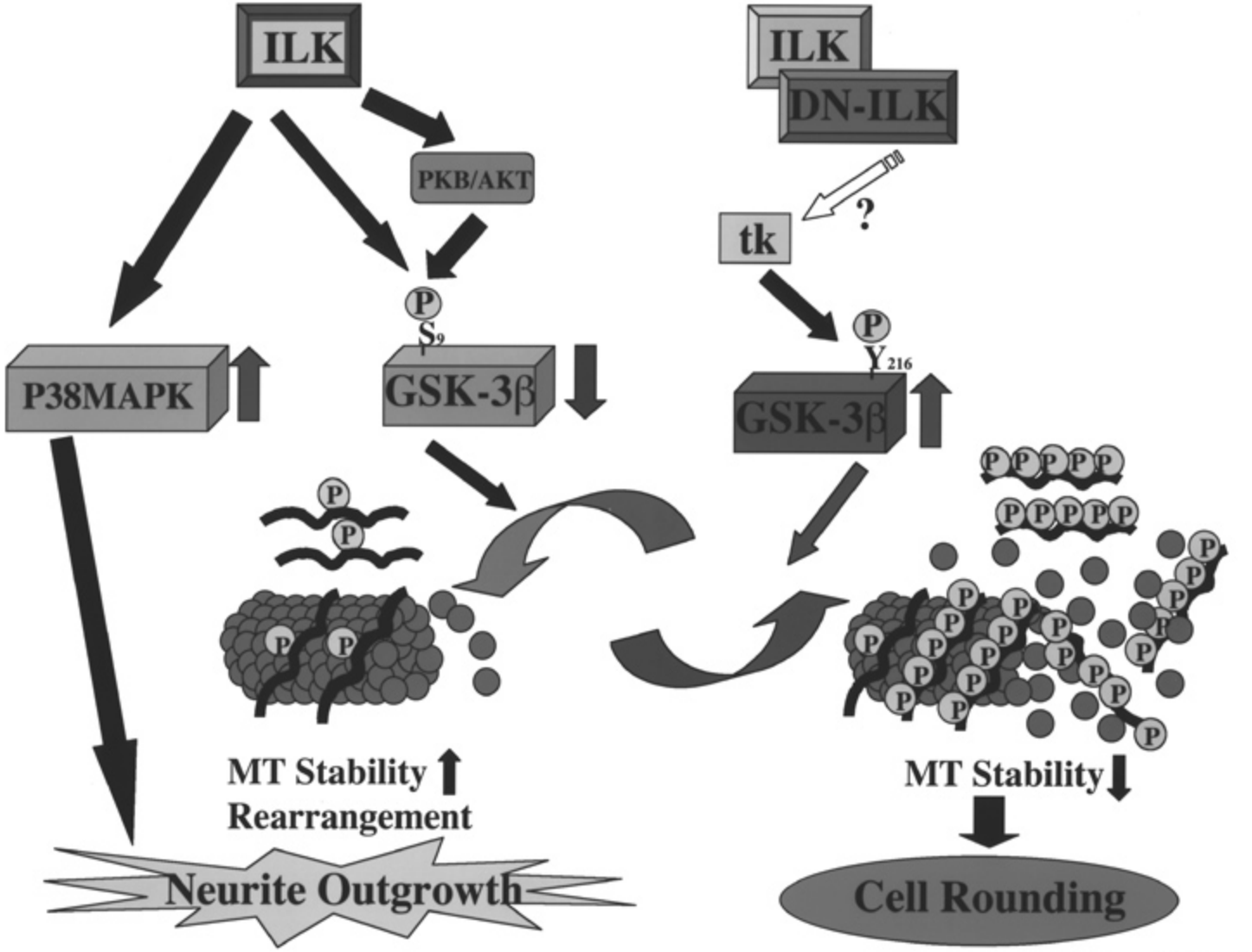

Ishii et al. Fig.6